



Characterization of maize amylose-extender (*ae*) mutant starches: Part II. Structures and properties of starch residues remaining after enzymatic hydrolysis at boiling-water temperature

Hongxin Jiang^a, Mark Campbell^b, Mike Blanco^c, Jay-Lin Jane^{a,*}

^a Department of Food Science and Human Nutrition, Iowa State University, Ames, IA 50011, USA

^b Truman State University, Kirksville, MO 63501, USA

^c USDA-ARS/Plant Introduction Research Unit, Ames, IA 50011, USA

ARTICLE INFO

Article history:

Received 31 August 2009

Received in revised form 19 October 2009

Accepted 26 October 2009

Available online 30 October 2009

Keywords:

Resistant starch

Starch structure

Amylose-extender mutant

High-amylose maize starch

Long-chain double-helical crystallite

ABSTRACT

GEMS-0067 maize *ae*-line starches developed by the Germplasm Enhancement of Maize (GEM) project consist of 39.4–43.2% resistant starch (RS), which is larger than the existing *ae*-line starches of H99*ae*, OH43*ae*, B89*ae*, and B84*ae* (11.5–19.1%) as reported in part I of the study. The objective of this study was to understand the mechanism of the RS formation in the GEMS-0067 *ae*-line starch. In the current study, we analyzed the structures and properties of the RS residues that remained after enzymatic hydrolysis of the *ae*-line starches at 95–100 °C. The RS residues consisted of two major components: large starch molecules of average degrees of polymerization (DP) 840–951 with a few branches and small starch molecules (average DP 59–74) with mostly linear chains. All the RS residues had a semi-crystalline structure with the B-type polymorph and displayed high onset (100.7–107.7 °C), peak (118.6–121.4 °C), and conclusion (139.7–158.8 °C) gelatinization temperatures. After the maize *ae*-mutant starches were defatted with methanol, the RS contents decreased to 27.8–28.9% for the GEMS-0067 *ae*-line starches and 9.0–11.0% for the existing *ae*-line starches. The RS residues were attributed to the presence of long-chain double-helical crystallites derived from amylose and the intermediate component (IC). These crystallites present in native *ae*-line starches had gelatinization temperatures above 100 °C and maintained the semi-crystalline structures after enzymatic hydrolysis at 95–100 °C.

© 2009 Elsevier Ltd. All rights reserved.

1. Introduction

This paper reports a continuing study on characterization of maize *ae*-mutant starches. Part I of the study reported molecular structures and properties of selected maize *ae*-mutant starches, which included three new lines derived from GEMS-0067 *ae*-line, designated as GSOH 1, GSOH 2, and GSOH 3, and four additional *ae*-lines, H99*ae*, OH43*ae*, B84*ae*, and B89*ae*, designated as “existing *ae*-lines” (Li, Jiang, Campbell, Blanco, & Jane, 2008). GEMS-0067 was developed by M. Campbell at Truman State University nursery in Kirksville, MO, working cooperatively with the GEM project in Ames, IA. GEMS-0067 was derived from an exotic tropical breeding cross designated as GUAT209:S13 with the accession Guatemala 209 crossed to a stiff-stalk line (S13) (Campbell, Jane, Pollak, Blanco, & O'Brien, 2007). GEMS-0067 is homozygous for the *ae* gene and is also known to have modifier genes for enhancing the level of amylose (Campbell et al., 2007).

The starches of GEMS-0067 *ae*-lines displayed significantly larger RS contents (39.4–43.2%) than that of the existing *ae*-lines (11.5–19.1%) determined using AOAC Method 991.43 for total dietary fiber (Li et al., 2008). RS contents of the starch samples, determined using Englyst's method (Englyst, Kingman, & Cummings, 1992) after cooking the starch at 100 °C for 30 min, also showed that GEMS-0067 *ae*-line starches had more RS (30.9–34.3%) than did the existing *ae*-line starches (18.6–20.9%) (Li et al., 2008). The GEMS-0067 *ae*-line starches had greater apparent-amylose contents (83.1–85.6%) and less amylopectin contents (10.7–13.9%) than did the existing *ae*-line starches (61.7–67.7% and 25.4–33.5%, respectively) (Li et al., 2008). The RS content was positively correlated with the apparent-amylose content of the maize *ae*-mutant starch ($r = .99$) (Li et al., 2008). The GEMS-0067 *ae*-line starches contained 36.1–45.0% IC, which were higher than the IC contents of most of the existing *ae*-line starches (22.4–27.0%) except OH43*ae* starch (52.0%) (Li et al., 2008). The average branch-chain-lengths of the IC molecules isolated from the maize *ae*-mutant starches varied from DP 31.6 to 50.6 (Li et al., 2008). The GEMS-0067 *ae*-line starches displayed higher conclusion gelatinization temperatures (122.0–130.0 °C) than did the existing

* Corresponding author. Tel.: +1 515 294 9892; fax: +1 515 294 8181.

E-mail address: jjane@iastate.edu (J.-L. Jane).

ae-line starches (100.5–105.3 °C) (Li et al., 2008). The authors proposed that the semi-crystalline structure of the GEMS-0067 *ae*-line starches remained after digesting with thermally stable α -amylase at 95–100 °C. Consequently, the GEMS-0067 *ae*-line starches displayed greater RS contents (Li et al., 2008).

Structures of RS obtained after enzymatic hydrolysis of high-amylose maize starches using pancreatic α -amylase at 37 °C have been reported (Evans & Thompson, 2004; Shi & Jeffcoat, 2001). On the basis of broad molecular-weight distributions of the RS residue, Shi and Jeffcoat (2001) concluded that both molecular structures and the granular structure of high-amylose maize starch granules contributed to the resistance of starch molecules to pancreatic α -amylase hydrolysis (Shi & Jeffcoat, 2001). Evans and Thompson (2004) reported that the RS residue had similar branch-chain-length profiles to the native high-amylose maize starch and proposed that the molecular organization in the high-amylose maize starch granule was the primary factor resulting in the enzyme resistance of starch (Evans & Thompson, 2004).

In the current study, we aimed to identify which starch components (amylose, IC, or amylopectin) remained in the RS residues, where they were located in the starch granule, and what types of physical structures they had by analyzing the chemical, physical, and morphological structures of the RS residues remaining after the thermal and enzymatic treatments. We also investigated how lipids in the starch affected the enzymatic hydrolysis of the starch. On the basis of these results, we proposed a mechanism of RS formation in the *ae*-line starches.

2. Materials and methods

2.1. Materials

Maize kernels of three new lines (F6 generation) derived from GEMS-0067 *ae*-lines, including GUAT209:S13 \times (OH43*ae* \times H99*ae*) B-B-4-1-2-1-1 (GSOH 1), GUAT209:S13 \times (OH43*ae* \times H99*ae*) B-B-4-4-2-1-1 (GSOH 2), and GUAT209:S13 \times (OH43*ae* \times H99*ae*) B-B-4-4-201-2 (GSOH 3), and four existing *ae*-lines H99*ae*, OH43*ae*, B89*ae*, and B84*ae* were produced at the Truman State University Farm (Kirkville, MO). All chemicals were reagent grade, obtained from Sigma–Aldrich Co. (St. Louis, MO) or Fisher Scientific (Pittsburgh, PA), and were used as received. Crystalline *Pseudomonas* isoamylase (EC 3.2.1.68) with specific activity about 66,000 units per milligram of protein was purchased from Hayashibara Biochemical Laboratories, Inc. (Okayama, Japan) and was used without further purification.

2.2. Starch isolation

Starch was isolated from maize kernels using the method reported by Li et al. (2008).

2.3. Removal of lipid

The lipid was removed according to the method reported by Schoch (1942). Starch (5.0 g) was placed in a Whatman Cellulose Extraction Thimble (22 mm I.D. \times 80 mm) and was defatted using methanol in a Soxhlet extractor for 24 h. The methanol of the extraction solution was removed using a rotary evaporator (Büchi/Brinkmann Rotavapor-R). The lipid residue was dried at 105 °C overnight. The content of the removed lipid was calculated as the amount of the dried lipid residue divided by the dry weight of the native starch. The defatted starches were dried at 37 °C for 24 h.

2.4. RS content

RS content was determined using AOAC Official Method 991.43 for total dietary fiber (AOAC, 2003) following the procedure reported by Li et al. (2008).

2.5. Starch morphology

Scanning electron microscopy (SEM) images of starch samples were taken using a scanning electron microscope (JEOL JSM-35, Tokyo, Japan) at the Microscopy and NanoImaging Facility, Iowa State University. The starch samples were coated with gold–palladium (60:40), and the SEM images were taken at 10 kV (Ao & Jane, 2007).

The percentage of rod/filamentous starch granules was determined using the number of rod/filamentous starch granules divided by the total number of starch granules shown on SEM images. At least 900 total starch granules were used for the calculation of the percentage. The short (S) and the long (L) axes of starch granules were measured using SIS Pro software (Soft Imaging System, Inc., Lakewood, CO), and the L/S ratios were calculated. Starch granules were considered as rod/filamentous granules when the L/S ratios were larger than 1.3.

2.6. Molecular-weight distributions of the RS residues

Molecular-weight distributions of the RS residues obtained after enzymatic hydrolysis of native *ae*-line starches at 95–100 °C (AOAC Method 991.43) were analyzed using a high-performance size-exclusion chromatograph (HPSEC) equipped with a refractive-index (RI) detector. The RS residue (20 mg) was wetted with water (0.2 mL), dispersed in dimethyl sulfoxide (DMSO) (1.8 mL) at 100 °C for 1 h and kept at room temperature with gentle mechanical stirring for 16 h, precipitated using ethanol (20 \times), collected, and then redissolved in boiling water with mechanical stir in a boiling-water bath for 30 min. An aliquot (100 μ L) of the dispersion was filtered through a nylon membrane (5 μ m pore size) following the method of Yoo and Jane (2002) with modifications. The HPSEC-RI system consisted of an isocratic pump (HP 1050, Hewlett–Packard, Valley Forge, PA), an injection valve (100 μ L sample loop, Model 7725, Rheodyne), and an RI detector (G1362A, Agilent, Santa Clara, CA). SB-806 and SB-804 analytical columns with a Shodex OH pak SB-G guard column (Showa Denko K.K., Tokyo, Japan) were used to analyze the molecular-weights of the RS residues. Milli-Q water (18 Ω) filtered through a membrane with a pore size of 0.02 μ m (Cat. No. 6809-5002, Whatman) was used as the eluent. Pullulan standards (P-5, P10, P20, P50, P100, P200, and P400, Showa Denko K.K., Tokyo, Japan) were used as references for the determination of molecular-weights of the RS residues.

The molecular-weight distributions of the RS residues were also analyzed using Sepharose CL-2B gel permeation chromatography (GPC), following the method of Jane and Chen (1992). Three peaks, designated as large (F1), medium (F2), and small (F3) molecular-weight fractions, were collected separately for further structural analysis of each of the RS molecules.

2.7. Molecular structures of the RS residues collected in the F2 fraction

The F2 fraction of the RS residue was collected and debranched following the method described by Li et al. (2008). The samples with and without debranching reaction were dispersed in DMSO (90%) at 100 °C, precipitated using ethanol (20 \times), collected, and then redissolved in hot water with stirring in a boiling-water bath for 30 min. An aliquot (20 μ L) of the dispersion was filtered through a nylon membrane (5 μ m pore size) and analyzed using a HPSEC equipped with an RI detector (HPSEC-RI). The HPSEC-RI

system consisted of a pump (Prostar 210, Varian, Walnut Creek, CA), an injection valve (20 μ L sample loop, Model 7725, Rheodyne), and an RI detector (Prostar 355, Varian, Walnut Creek, CA). A SB-803 analytical column with a Shodex OH pak SB-G guard column (Showa Denko K.K., Tokyo, Japan) was used to determine the molecular-weights of the samples. The temperature of the columns was maintained at 50.0 $^{\circ}$ C using a column oven (Model 510, Varian, Walnut Creek, CA). The temperature of the RI detector was set at 35.0 $^{\circ}$ C. The eluent was distilled–deionized water filtered through a membrane with pore size of 0.45 μ m. Maltopentaose, maltohexa-

ose, maltoheptaose, and the same pullulan standards described in 2.6 were used for molecular-weight calibration.

2.8. Molecular structures and chain-length distributions of the RS residues collected in the F3 fraction

The molecular-weight distributions of the RS residues collected in the F3 fraction, before and after isoamylase-debranching, were determined using a GPC column packed with Bio-Gel P-30 gel (1.5 I.D. \times 50 cm) (Bio-Rad Laboratories, Richmond, CA). The eluent

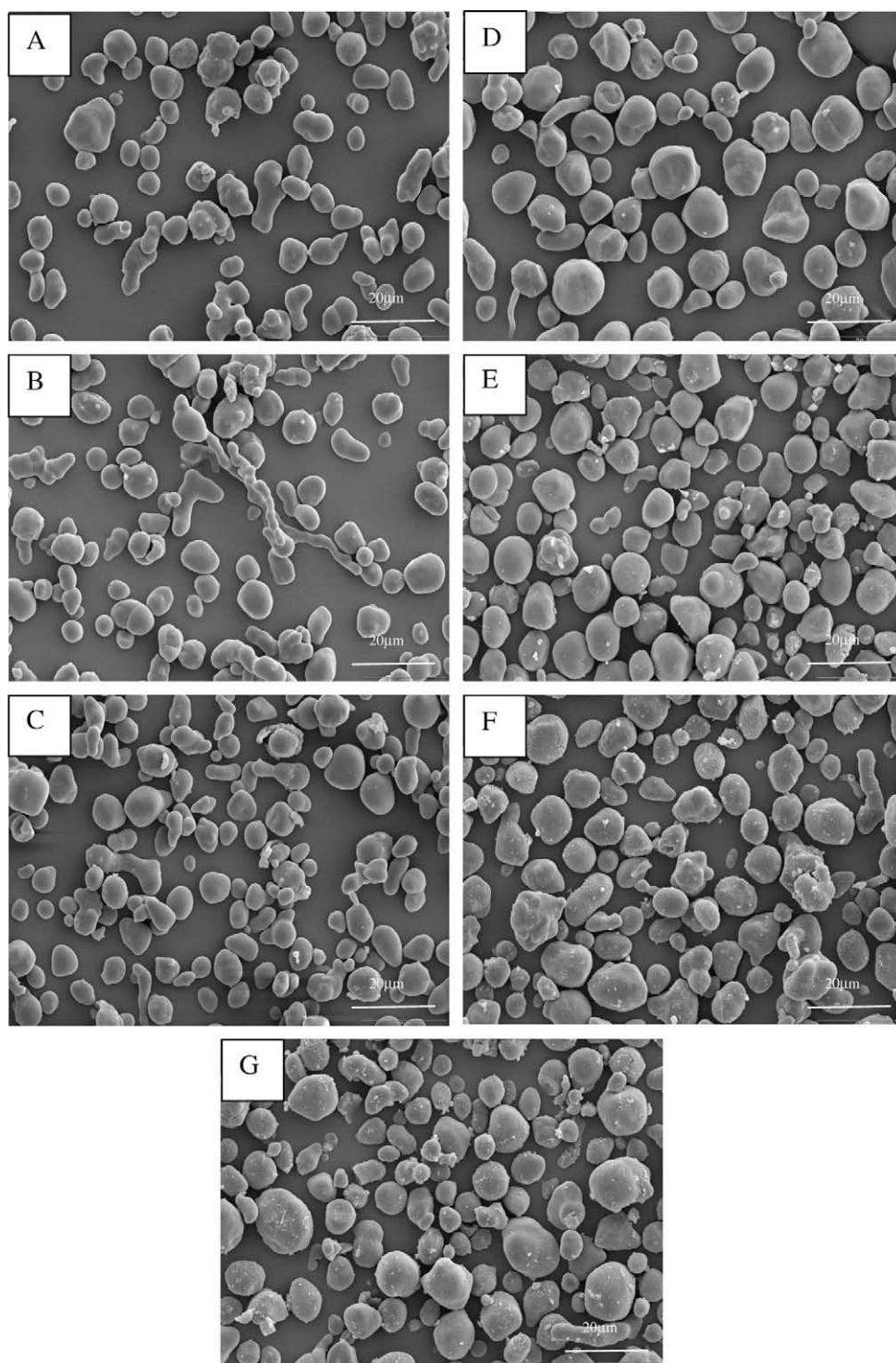


Fig. 1. SEM images of native maize *ae*-mutant starches. (A) GSOH 1, (B) GSOH 2, (C) GSOH 3, (D) H99ae, (E) OH43ae, (F) B89ae, and (G) B84ae.

Table 1
Proportions of rod/filamentous granules, lipid extracted, and RS content in maize *ae*-mutant starches.

Sample	Proportions of rod/filamentous granules (%)	Lipid extracted ^a (%)	RS ^b (%)	
			Before defatting	After defatting ^a
GSOH 1	32.0 ± 0.0	0.69 ± 0.05	41.5 ± 2.0	28.9 ± 0.4
GSOH 2	30.2 ± 2.4	0.59 ± 0.03	43.4 ± 3.2	27.8 ± 2.8
GSOH 3	22.6 ± 1.0	0.64 ± 0.03	37.3 ± 0.7	27.8 ± 0.2
H99 <i>ae</i>	7.7 ± 0.6	0.38 ± 0.03	13.0 ± 0.3	11.0 ± 0.9
OH43 <i>ae</i>	5.6 ± 0.4	0.41 ± 0.02	14.0 ± 0.5	10.9 ± 0.3
B89 <i>ae</i>	7.5 ± 0.8	0.23 ± 0.02	14.9 ± 0.4	9.3 ± 0.3
B84 <i>ae</i>	5.2 ± 0.9	0.41 ± 0.01	10.6 ± 1.4	9.0 ± 0.7

^a Extraction of lipids was done using methanol in a Soxhlet extractor for 24 h.^b The RS content was determined using AOAC Method 991.43 for total dietary fiber.

was a sodium-chloride aqueous solution (25 mM) containing sodium hydroxide (pH adjusted to 9.8). The column was run in a descending mode with a flow rate of 18 mL/h. Fractions of 2.0 mL each were collected and analyzed for total carbohydrate content using the phenol-sulfuric acid method (Dubois, Gilles, Hamilton, Rebers, & Smith, 1956).

The isoamylase-debranched F3 starch was also analyzed for the chain-length distribution using a fluorophore-assisted capillary-electrophoresis (FACE) following the procedure of Morell, Samuel, and O'Shea (1998) with modifications. The debranched sample was adjusted to pH 7, boiled for 15 min, and filtered through a membrane filter (1.2 µm pore size). The filtrate (80 µL, 2 mg/mL) was dried at 45 °C using a centrifugal vacuum evaporator for 3 h. Two microliters of 8-aminopyrene-1,3,6-trisulfonic acid (APTS, Cat. No. 09341, Sigma, St. Louis, MO) solution (0.2 M APTS in 15% acetic acid) and 2 µL of sodium cyanoborohydride (1 M in tetrahy-

drofuran, Cat. No. 296813, Sigma, St. Louis, MO) were added to the dried sample. The mixture was incubated at 40 °C for 16 h. The APTS-labeled sample was injected into the FACE system (P/ACE MDQ, Beckman Coulter, Fullerton, CA) at 0.5 psi for 5 s. A N-CHO coated capillary tubing (50 µm I.D., 50 cm length, Cat. No. 477601, Beckman Coulter, Fullerton, CA) was used to separate APTS-labeled molecules. The separation was performed at 23.5 kV at 25 °C.

2.9. Starch crystallinity

Starch samples were equilibrated in a chamber with 100% relative humidity at 25 °C for 24 h. X-ray diffraction patterns of the starch samples were determined using a diffractometer (D-500, Siemens, Madison, WI) with copper K α radiation (Ao & Jane, 2007). Crystallinity of the starch was calculated using the following

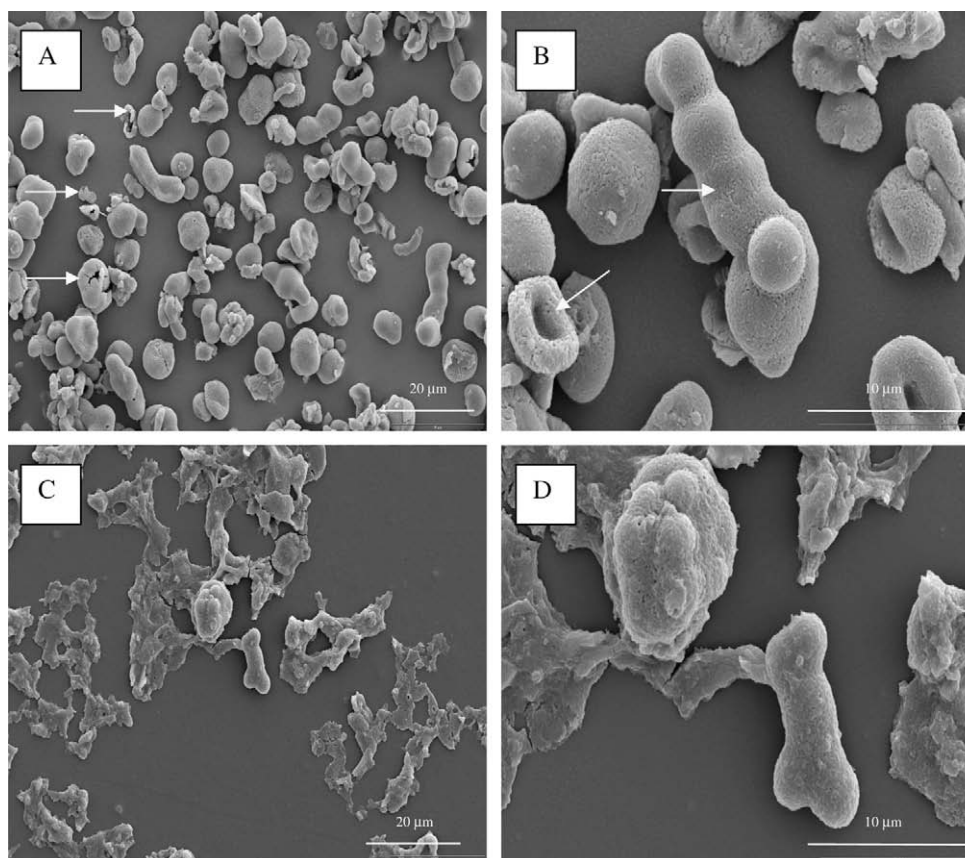


Fig. 2. Selected SEM images of the RS residues collected after enzymatic hydrolysis at 95–100 °C (AOAC Method 991.43). A (1500 \times) and B (5000 \times): RS residue of GEMS-0067; C (1500 \times) and D (5000 \times): RS residue of B89*ae*. Arrows indicate fragmented, hollowed and half-shell-like granules and starch granule retained the shape.

equation. Crystallinity (%) = $100A_c/(A_c + A_a)$, where A_c is the crystalline area on the X-ray diffractogram and A_a is the amorphous area.

2.10. Thermal properties of the RS residues

Thermal properties of the RS residues were analyzed using a differential scanning calorimeter (DSC) (DSC-7, Perkin-Elmer, Nor-

walk, CT) (Kasemsuwan, Jane, Schnable, Stinard, & Robertson, 1995). Starch (~6.0 mg, dry basis) was precisely weighed in a stainless steel pan, mixed with ~18 μ L of distilled water. The pan was sealed, equilibrated at room temperature for 1 h, and then heated at a rate of 10 °C/min from 10 to 180 °C. A sealed empty pan was used as the reference. Onset (T_o), peak (T_p), and conclusion (T_c) temperatures and enthalpy change (ΔH) of starch gelatiniza-

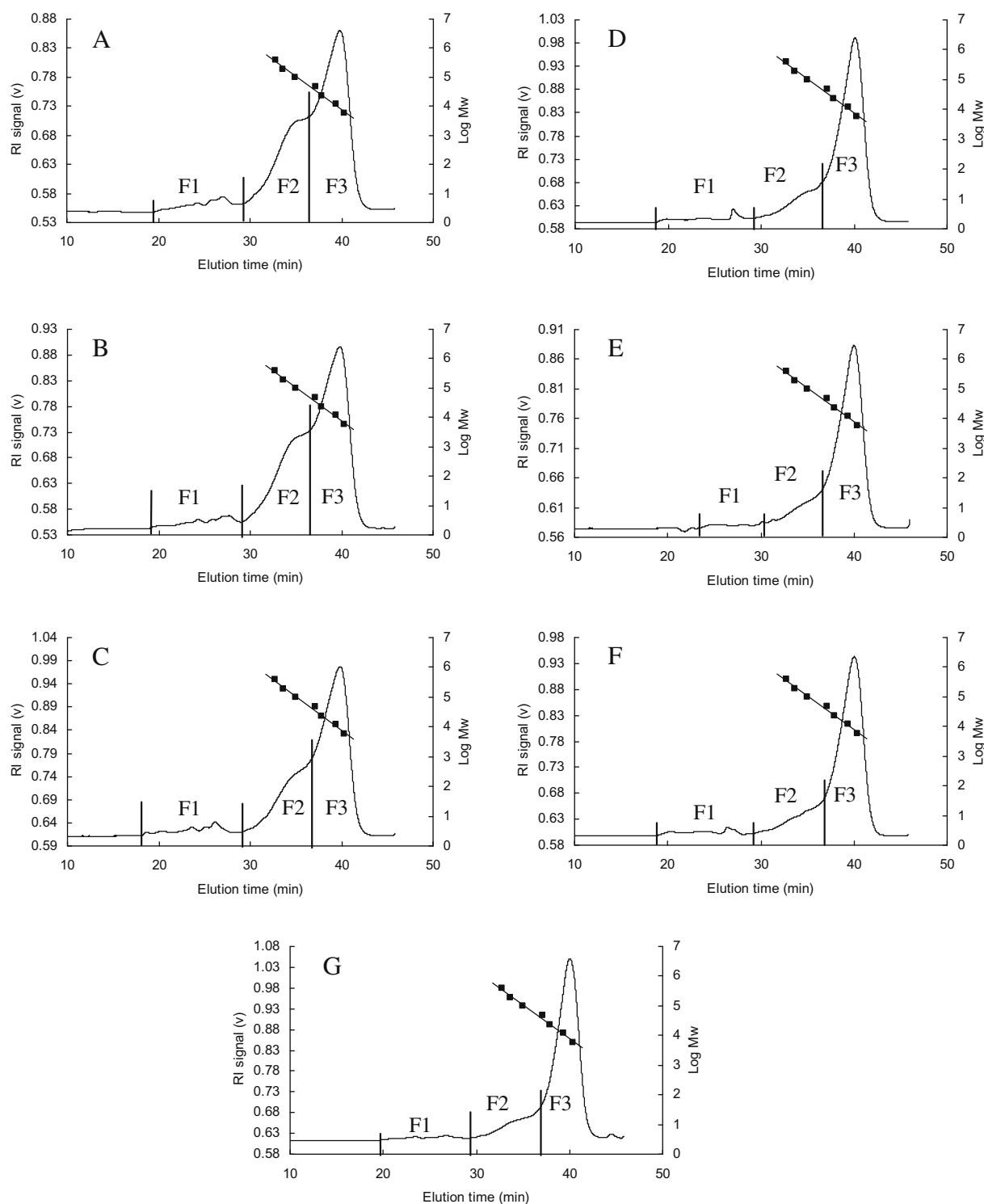


Fig. 3. High-performance size-exclusion chromatograms of the RS residues determined using analytical columns SB-806 and SB-804 (Showa Denko K.K., Tokyo, Japan). The RS residues were dispersed in DMSO (90%) at 100 °C, precipitated using ethanol (20 \times), collected, and then redissolved in hot water. Milli-Q water was used as eluent. (A) GSOH 1, (B) GSOH 2, (C) GSOH 3, (D) H99ae, (E) OH43ae, (F) B89ae, and (G) B84ae. —■—, a pullulan standard curve with molecular-weights of DP 36, 73, 146, 292, 617, 1148, and 2472. F1, F2, and F3 were large, medium, and small molecular-weight fractions of RS residues, respectively.

Table 2
Average molecular-weights (MW) of the RS residues collected in the F2 and F3 fractions.^{a,b}

Sample	Ratio (%)			MW of F2 (DP)			MW of F3 (DP)
				Before debranching		After debranching	
	F1	F2	F3		P1	P2	
GOSH 1	5.5	36.9	57.6	951	547	57	72
GOSH 2	5.2	37.9	56.9	944	648	60	74
GOSH 3	5.0	30.8	64.2	864	675	59	69
H99 <i>ae</i>	2.9	20.2	76.9	870	491	53	61
OH43 <i>ae</i>	2.3	19.2	78.4	870	422	47	63
B89 <i>ae</i>	4.3	18.2	77.5	883	411	47	62
B84 <i>ae</i>	3.9	14.7	81.4	840	98	17	59

^a F1, F2, and F3 were large, medium, and small molecular-weight fractions of RS residues, respectively.

^b DP, degree of polymerization; P1 and P2 are two peaks of debranched F2 starch.

tion were calculated using Pyris software (Perkin-Elmer, Norwalk, CT).

3. Results and discussion

3.1. Morphology of native maize *ae*-mutant starches and their RS residues

SEM images of native maize *ae*-mutant starches are shown in Fig. 1. All the native *ae*-mutant starches consisted of mainly two types of starch granules: spherical granules and rod/filamentous granules. The rod/filamentous granules displayed shapes of rod, filament, triangle, socks, etc. (Fig. 1A–G). Some filamentous granules were more than 50 μm long (Fig. 1B). Starches of the GEMS-0067 *ae*-lines consisted of substantially larger proportions of rod/filamentous granules (22.6–32.0%) (Table 1 and Fig. 1A–C) than that of the existing *ae*-lines (5.2–7.7%) (Table 1 and Fig. 1D–G). The proportion of rod/filamentous granules increased with the increase in apparent-amylose content of the maize *ae*-mutant starch ($r = .98$, $p < .05$). Apparent-amylose contents are 83.1–85.6% for the GEMS-0067 *ae*-line and 61.7–67.7% for the existing *ae*-line starches reported by Li et al. (2008). Many studies have reported the presence of rod/filamentous granules in maize *ae*-mutant starches, but none have shown such large proportions as observed in the GEMS-0067 *ae*-line starches (Boyer, Daniels, & Shannon, 1976; Mercier, Charbonniere, Gallant, & Guilbot, 1970; Shi & Jeffcoat, 2001; Sidebottom, Kirkland, Strongitharm, & Jeffcoat, 1998; Wolf, Seckinger, & Dimler, 1964).

Representative SEM images of the RS residues collected after α -amylase hydrolysis of the starches at 95–100 °C (AOAC Method 991.43) are shown in Fig. 2. Fragmented, hollowed, and half-shell-like granules and granules retaining the original shape were observed in the RS residues of GEMS-0067 *ae*-line starches (Figs. 2A and B). Granules that retained the native shape were mostly rod/filamentous starch granules, and there were many such granules observed in the RS residues of GEMS-0067 *ae*-line starches (Fig. 2A and B). There was little or no gel-like starch in the RS residues of GEMS-0067 *ae*-line starches. The RS residues of the existing *ae*-line starches, however, were mostly in a gel-like form (Fig. 2C and D).

The hollowed and half-shell-like granules observed in the RS residues of GEMS-0067 *ae*-lines (Fig. 2A and B) and the gel-like starch in the RS residues of the existing *ae*-lines (Fig. 2C and D) were likely the remnants of the outer layer of spherical granules, which consisted of more amylose as reported previously (Jane & Shen, 1993; Li, Blanco, & Jane, 2007; Pan & Jane, 2000). It is plausible that starch molecules around the hilum were promptly gelatinized and hydrolyzed because the starch molecules around the hilum were loosely packed and had less amylose (Gray & BeMiller, 2004; Huber & BeMiller, 2001; Jane & Shen, 1993; Li et al., 2007;

Pan & Jane, 2000). All the SEM results (Fig. 2A–D) showed that the RS was more concentrated in rod/filamentous starch granules and at the outer layer of the spherical starch granule.

3.2. Effect of lipid on the RS content

The amounts of lipids extracted from the native starch samples using methanol were 0.59–0.69% (dry starch basis, dsb) for GEMS-0067 *ae*-line starches and 0.23–0.41% (dsb) for the existing *ae*-line starches (Table 1). The RS contents of the methanol-defatted starches of the GEMS-0067 *ae*-lines (27.8–28.9%) were substantially less than that of the native starches without defatting (37.3–43.4%) (Table 1). The RS contents of the existing *ae*-line starches after defatting (9.0–11.0%) were also decreased from that of the native starches (10.6–14.9%) (Table 1). These results showed that lipids in the native maize *ae*-mutant starches reduced enzymatic digestibility of starch at 95–100 °C.

3.3. Molecular-weight distributions of the RS residues

Molecular-weight distributions of the RS residues remaining after the thermal treatment at 95–100 °C and enzymatic hydrolysis, analyzed using HPSEC-RI, are shown in Fig. 3. The amylopectin molecules (peak eluted between 18.4 and 22.4 min) were hydrolyzed to smaller molecules, and the amylopectin peak disappeared after the thermal and enzymatic treatments (Fig. 3). The residual RS showed three peaks in the chromatograms, which were divided and designated as F1 (average DP $\sim 3.47 \times 10^5$), F2 (average DP 840–951), and F3 (average DP 59–74) (Fig. 3 and Table 2). The ratios of F1:F2:F3 are summarized in Table 2. All the RS residues contained small amounts of F1 starch (2.3–5.5%), which were likely partially hydrolyzed amylopectin. The RS residues obtained from the GEMS-0067 *ae*-line starches consisted of larger proportions of F2 starch (30.8–37.9%) than those obtained from the existing *ae*-line starches (14.7–20.2%).

Sephacose CL-2B chromatograms of the RS residues were similar to the HPSEC-RI chromatograms of the RS residues shown in Fig. 3. Thus, the chromatograms of the Sephacose CL-2B are not shown. F1, F2, and F3 fractions separated by the Sephacose CL-2B column were collected separately and used for the structural analysis of starch molecules.

3.4. Molecular structures of the RS residues collected in the F2 fraction

Molecules collected in the F2 fraction separated by the Sephacose CL-2B column were debranched to determine the branch structures of the F2 starch molecules. The molecular-weight distributions of the F2 starch molecules, before and after isoamylase-debranching, are shown in Fig. 4. Before the debranching reaction, the F2 starch molecules showed one major peak and some

minor peaks of molecular-weights larger than DP 2827 (eluted before 15 min) with an exception of B84ae. After the isoamylase-debranching reaction of the F2 starch, the minor peaks of large molecules (>DP 2827) disappeared, suggesting those large molecules being highly branched partially hydrolyzed amylopectin and IC molecules. The chromatograms showed two major peaks, designated as P1 and P2 (Fig. 4). The average molecular-weights of the P1 and P2 of the GEMS-0067 ae-lines (DP 547–675 and DP 57–60, respectively) were larger than that of the H99ae, OH43ae,

and B89ae (DP 411–491 and DP 47–53, respectively) and B84ae (DP 98 and 17, respectively) (Table 2). The large linear-molecules of the P1 obtained from GEMS-0067 ae-line starches and the majority of the existing ae-line starches resembled the structures of amylose molecules.

The debranched F2 starch of the B84ae RS residue consisted of mainly short-chain molecules of DP 98 and 17 for P1 and P2, respectively (Fig. 4G and Table 2). The lack of large amylose-like molecules in the debranched F2 starch of the B84ae RS residue (Ta-

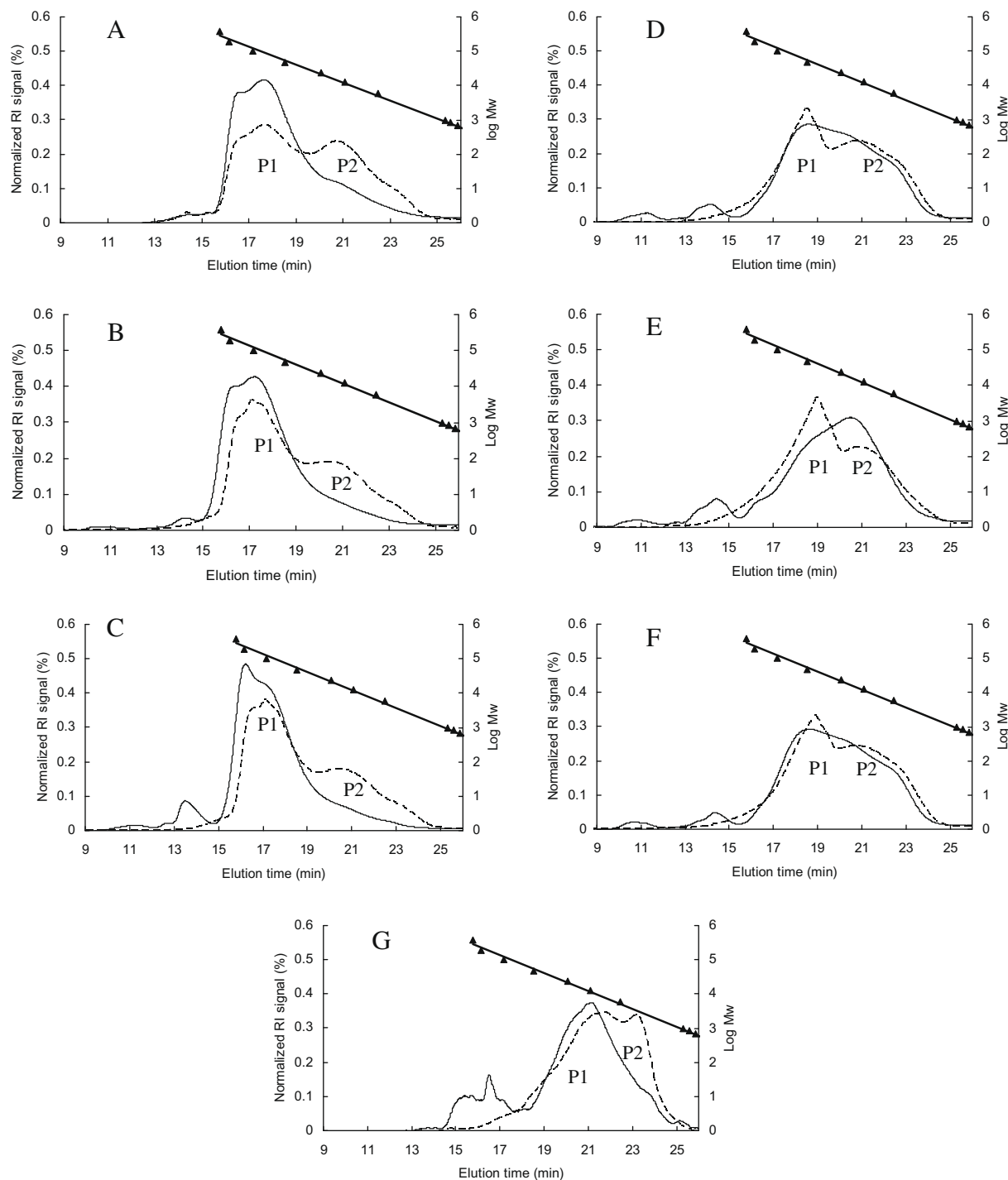


Fig. 4. High-performance size-exclusion chromatograms of the RS residues collected in the F2 fraction. The separation was conducted using a SB-803 analytical column (Showa Denko K.K., Tokyo, Japan). (A) GSOH 1, (B) GSOH 2, (C) GSOH 3, (D) H99ae, (E) OH43ae, (F) B89ae, and (G) B84ae. —, before debranching; ----, after debranching; —▲—, a standard curve of maltopentaose (DP 5), maltohexaose (DP 6), maltoheptaose (DP 7), and pullulan standards (DP 36, 73, 146, 292, 617, 1148, and 2472). P1 and P2, peaks of debranched F2 starch molecules.

ble 2) coincided with the lowest RS content (10.6%) (Table 1) and the lowest conclusion gelatinization temperature ($T_c = 100.5^\circ\text{C}$) of the B84ae starch among all the ae-line starch samples tested (Li et al., 2008). Therefore, the B84ae starch was considered to have a different structure from others and will be discussed separately.

The average molecular-weights (DP 864–951) of the F2 starches obtained from all the samples except B84ae (Table 2) were similar to

that of the amyloses isolated from GEMS-0067 ae-line and H99ae starches (DP 817 and DP 756, respectively) and from other high-amylose maize starches (DP 690–740) (Jane & Chen, 1992; Takeda, Takeda, & Hizukuri, 1989). The average molecular-weights of the P1 and P2 of the debranched F2 starches (Table 2), however, were smaller than that of the two major peaks of debranched amyloses isolated from the GEMS-0067 ae-line starch (DP 1359 and 143, respectively) and from the H99ae starch (DP 1200 and 156, respec-

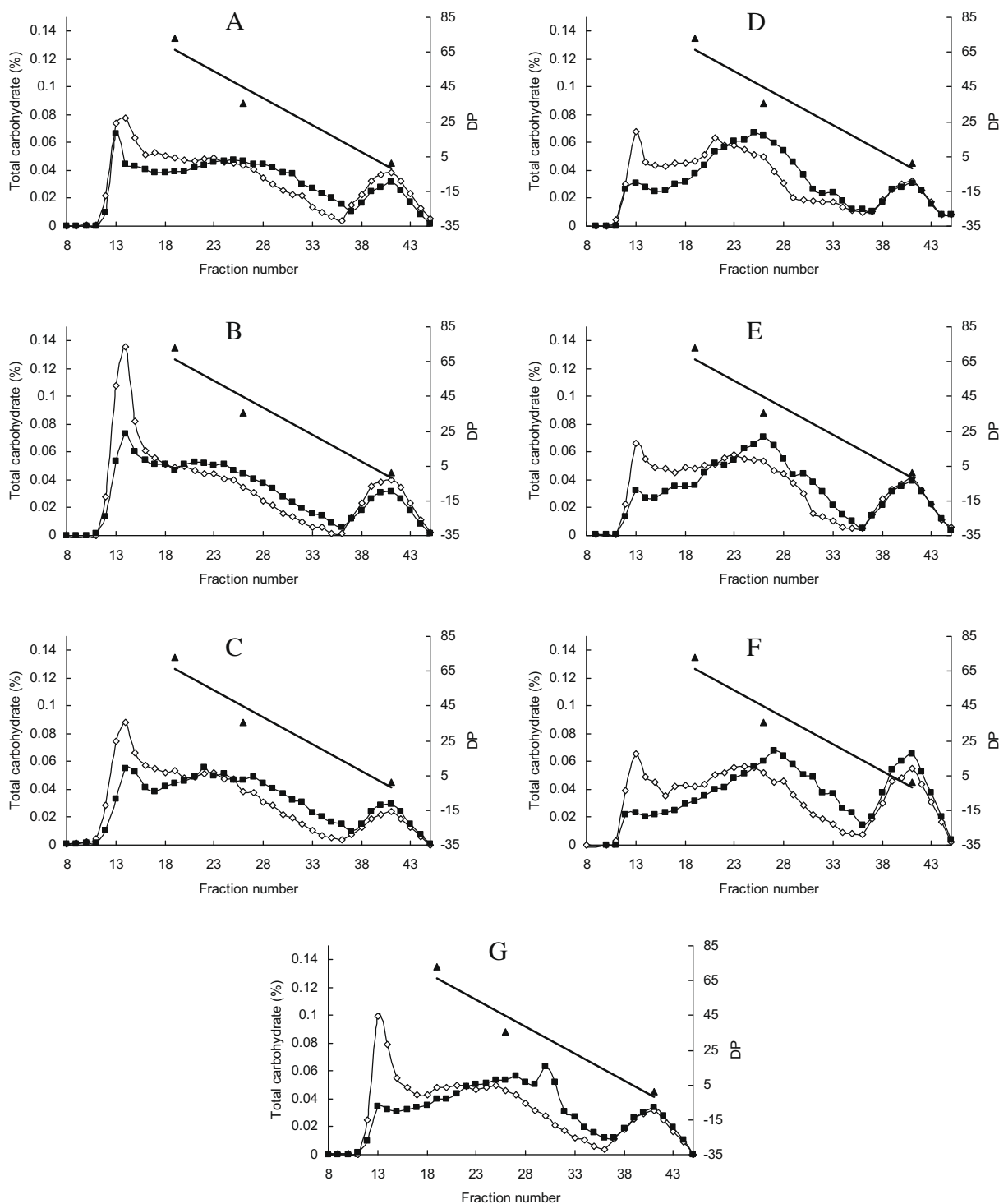


Fig. 5. Gel-permeation chromatograms of the RS residues collected in the F3 fraction determined using Bio-Gel P-30 gel (Bio-Rad Laboratories, Richmond, CA). (A) GSOH 1, (B) GSOH 2, (C) GSOH 3, (D) H99ae, (E) OH43ae, (F) B89ae, and (G) B84ae. \diamond —, before debranching; \blacksquare —, after debranching; \blacktriangle —, a standard curve of glucose and pullulan standards (DP 36 and 73). The glucose was used as an internal reference and eluted between 37 and 45 fractions.

tively). These results suggested presence of partially hydrolyzed amylose, IC, or amylopectin molecules in the F2 fraction. The presence of partially hydrolyzed amylose molecules was evident by the average molecular-weights of the P1 linear-molecules (DP 411–675) smaller than that of the major peak of the debranched amyloses of GEMS-0067 *ae*-line (DP 1359) and H99*ae* (DP 1200). The presence of the partially hydrolyzed IC and amylopectin molecules in the F2 starches was evident by the disappearance of the minor peak (DP > 2827) of the F2 starches after the isoamylase-

debranching reaction (Fig. 4) and the average molecular-weights of the P2 (DP 47–60) of the debranched F2 starches (Table 2). The presence of the partially hydrolyzed amylose, IC, and amylopectin molecules in the F2 fraction could be resulted from the fact that amylose and some IC and amylopectin molecules formed long-chain double-helical crystallites having gelatinization temperature above 95–100 °C. These long-chain double-helical crystallites formed a block and protected the bulk of the amylose and parts of IC and amylopectin molecules from enzymatic hydrolysis at 95–100 °C.

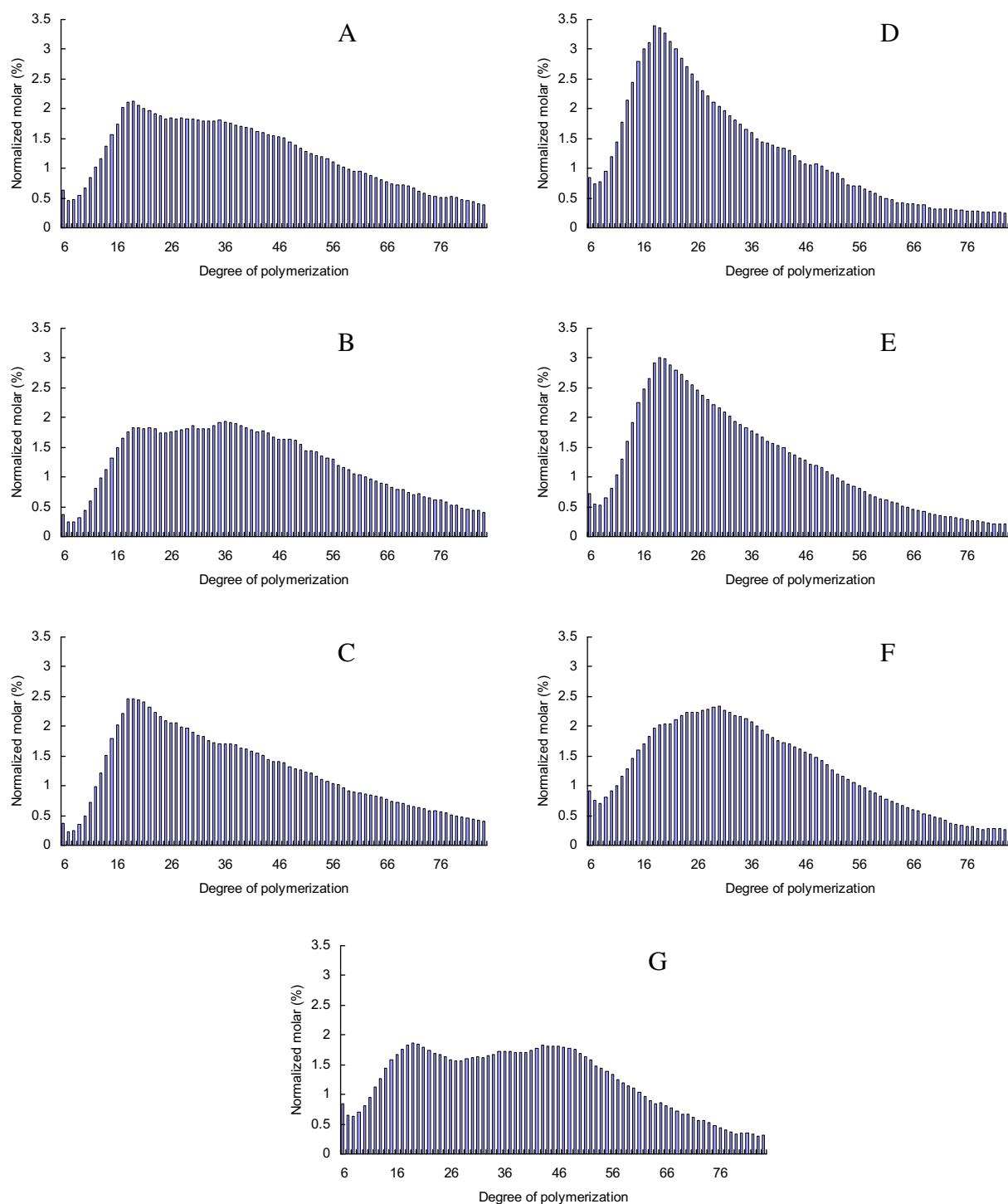


Fig. 6. Molar-based chain-length distributions of the debranched RS residues collected in the F3 fraction determined using FACE. (A) GSOH 1, (B) GSOH 2, (C) GSOH 3, (D) H99*ae*, (E) OH43*ae*, (F) B89*ae*, and (G) B84*ae*.

3.5. Molecular structures and chain-length distributions of the RS residues collected in the F3 fraction

The molecular-weight distributions of starch molecules in the F3 fraction determined using GPC, with and without isoamylase-debranching, are shown in Fig. 5. Most of the F3 starch molecules were linear and could not be debranched except some large F3 starch molecules ($DP > \sim 73$) that were debranched by isoamylase and produced smaller linear-molecules (Fig. 5). The chain-length distribution of the debranched F3 starch was also determined using FACE (Fig. 6). FACE is powerful in determining the molecular-weight distribution of individual small linear-molecules, but it has a limited maximum detectable chain-length at about DP 80. The chain-length distributions of the debranched F3 starch molecules, both on molar and mass bases, are summarized in Table 3. The debranched F3 starches showed larger proportions of chains with $DP > 25$ (77.0–90.6%, mass-based) (Table 3 and Fig. 6) than did the debranched amylopectins (50.4–55.5%), large molecular-weight IC (52.8–65.0%), and most small molecular-weight IC (67.8–89.3%) (Li et al., 2008). These results suggested that the F3 starch molecules could consist of the residues of amylose, IC, and amylopectin molecules resulting from enzymatic hydrolysis of semi-crystalline amylose and branch-chains of IC and amylopectin. The remaining fragments of crystalline amylose after *Bacillus subtilis* α -amylase hydrolysis have average molecular-weight of DP 50 ranging from DP 45 to 65 (Jane & Robyt, 1984).

3.6. Thermal properties of the RS residues

Despite the large differences in the contents of the RS residues remaining after enzymatic hydrolysis of the maize *ae*-line starches (Table 1), all the RS residues displayed similar gelatinization temperatures (100.7–107.7 °C, 118.6–121.4 °C, and 139.7–158.8 °C for T_o , T_p , and T_c , respectively) (Table 4), which were higher than their native starch counterparts (Li et al., 2008), but lower than the RS residues obtained from retrograded amylose (120.4–125.5 °C, 148.1–157.7 °C, and 166.5–177.0 °C, respectively) reported by Sievert and Pomeranz (1990). The high onset gelatinization temperatures of the RS residues (above 100.7 °C) (Table 4) indicated the presence of long-chain double-helical crystallites in the RS residues. These long-chain double-helical crystallites retained semi-crystalline structures after heating at 95–100 °C and enzymatic hydrolysis.

The significant increase in the T_o from ~ 65 °C of the native starches to >100 °C of the RS residues was attributed to the gelatinization and hydrolysis of amylopectin that had a low gelatinization temperature. The increase in the T_c from ~ 100 °C (existing *ae*-lines) or ~ 125 °C (GEMS-0067 *ae*-lines) of the native starches to ~ 145 °C of the RS residues could be the result of removal of non-resistant starch. It was plausible that RS crystallites were present in the native starch but at low concentrations, which were below the threshold of the DSC detector. To test this hypothesis, we ran DSC thermograms of mixtures of the native starch and RS residue. The gelatinization thermogram of a mixture of 90% GEMS-0067 *ae*-line starch and 10% RS residue appeared similar to that of the native starch (data not shown). More studies will be conducted to further understand the increase in the conclusion gelatinization temperature of the RS residues.

3.7. Crystalline structures and RS formation

All the native maize *ae*-mutant starches displayed the B-type X-ray diffraction pattern (Fig. 7A), which was in agreement with the results reported by Shi, Capitani, Trzasko, and Jeffcoat (1998). Although the amylopectin contents were 10.7–13.9% for the

GEMS-0067 *ae*-line starches (Li et al., 2008), the percentage crystallinity of those starches were 22.8–26.1% (Fig. 7A). These results clearly indicated that some amylose/IC molecules of the GEMS-0067 *ae*-line starches were also present in the double-helical crystalline structure in the starch granules, which contributed to the total percentage crystallinity. In normal starch granules, it is known that amylopectin molecules are in the crystalline structure, whereas amylose molecules are present in amorphous (French, 1984; Jane, Xu, Radosavljevic, & Seib, 1992). It was likely that amylose molecules, the dominant component in the granule of the *ae*-

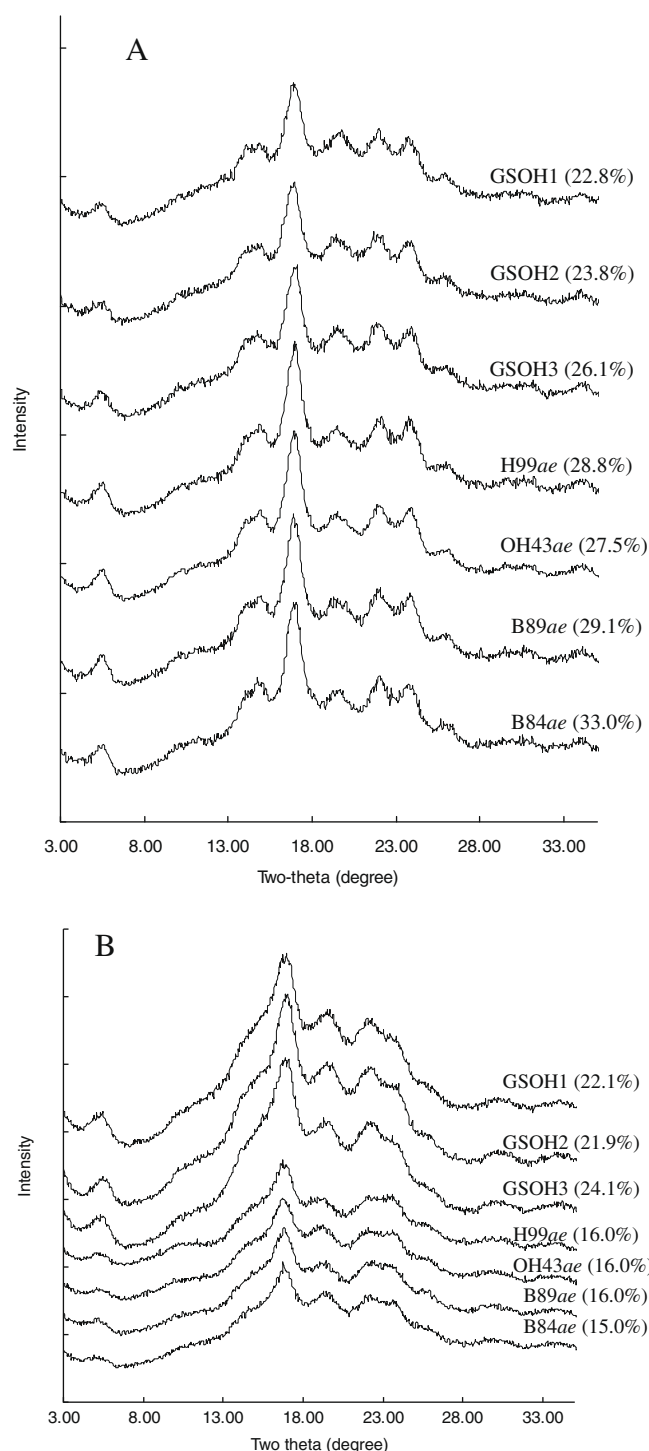


Fig. 7. X-ray diffraction patterns of (A) native starches and (B) RS residues. Crystallinity (%) is given in parentheses.

Table 3Molar-based chain-length distributions of the debranched RS residues collected in the F3 fraction.^a

Sample	Average CL (DP) ^b	DP ≤ 12 (%)	DP 13–24 (%)	DP 25–36 (%)	DP ≥ 37 (%)
GSOH 1	40.3 (50.7)	4.5 ± 0.2 (1.1) ^c	22.1 ± 0.2 (10.4)	22.5 ± 1.1 (17.0)	50.8 ± 1.2 (71.5)
GSOH 2	41.9 (51.2)	2.9 ± 0.2 (0.7)	19.0 ± 0.2 (8.7)	22.4 ± 0.7 (16.3)	55.5 ± 0.6 (74.3)
GSOH 3	39.2 (49.5)	3.4 ± 0.0 (0.9)	25.7 ± 0.6 (12.4)	23.0 ± 0.6 (17.8)	47.6 ± 1.6 (68.9)
H99ae	31.8 (41.1)	7.7 ± 0.1 (2.3)	35.1 ± 0.1 (20.7)	24.7 ± 0.5 (23.3)	32.5 ± 0.3 (53.7)
OH43ae	34.4 (43.7)	5.4 ± 0.2 (1.5)	30.7 ± 0.2 (16.9)	25.9 ± 0.4 (22.7)	38.0 ± 0.0 (58.9)
B89ae	35.7 (44.2)	6.6 ± 0.5 (1.7)	23.4 ± 1.2 (12.4)	26.9 ± 0.3 (22.9)	43.1 ± 2.0 (63.0)
B84ae	40.2 (49.8)	5.6 ± 0.1 (1.3)	20.1 ± 0.1 (9.4)	20.0 ± 0.6 (15.2)	54.3 ± 0.6 (74.1)

^a Molar-based chain-length distribution of the debranched RS residue was analyzed using FACE.^b DP, degree of polymerization.^c The number in the parenthesis is mass-based percentage of chain-lengths of the debranched RS residue.**Table 4**Thermal properties of the RS residues.^a

Sample	Gelatinization			
	T _o (°C)	T _p (°C)	T _c (°C)	ΔH (J/g)
GOSH 1	107.7 ± 0.3	120.5 ± 0.3	148.5 ± 0.7	14.4 ± 1.2
GOSH 2	107.1 ± 1.1	119.3 ± 0.5	139.7 ± 2.8	15.6 ± 1.5
GOSH 3	107.3 ± 1.6	121.3 ± 0.8	143.5 ± 0.7	16.6 ± 1.2
H99ae	101.2 ± 1.2	119.6 ± 1.7	145.8 ± 2.4	14.3 ± 1.5
OH43ae	102.9 ± 2.2	118.6 ± 2.0	142.7 ± 0.8	12.2 ± 1.4
B89ae	100.7 ± 0.2	121.4 ± 1.5	158.8 ± 1.6	25.7 ± 0.1
B84ae	100.8 ± 0.4	121.1 ± 0.1	145.6 ± 1.9	22.0 ± 0.0

^a T_o, T_p, T_c, and ΔH are onset temperature, peak temperature, conclusion temperature, and enthalpy change, respectively.

line starch, were not separated by amylopectin molecules and, thus, interacted with one another and formed the double-helical crystalline structure during the development of the starch granule. This finding was supported by the presence of partially preserved amylose molecules in the F2 fraction of the RS residues (Table 2 and Fig. 4), mostly linear chains up to >DP ~ 73 in the F3 fraction of the RS residues (Fig. 5), and the high conclusion gelatinization temperatures (100.5–130.0 °C) for the *ae*-line starches (Li et al., 2008).

Because RS content decreases with the increase in the amylopectin content of *ae*-line starch (Li et al., 2008), it is likely that the long-chain double-helical crystallites were mainly derived from amylose and IC, which had gelatinization temperatures above 100 °C (Table 4). These long-chain double-helical crystallites retained the semi-crystalline structures at 95–100 °C and were resistant to the enzymatic hydrolysis during the thermal treatment.

All the RS residues also displayed the B-type X-ray diffraction pattern with percentage crystallinity ranging from 21.9% to 24.1% for the GEMS-0067 *ae*-lines and 15.0–16.0% for the existing *ae*-lines (Fig. 7B). The decrease in the percentage crystallinity of the existing *ae*-line RS residues, from 27.5% to 33.0% of the native starches (Fig. 7A) to 15.0–16.0% of the RS residues (Fig. 7B), could be attributed to the hydrolysis of amylopectin in the starch granule. The existing *ae*-line starch consisted of substantially more amylopectin (25.4–33.5%) than the GEMS-0067 *ae*-line starch (10.7–13.9%) (Li et al., 2008). The percentages of crystallinity observed for the RS residues of the GEMS-0067 *ae*-line starch and the existing *ae*-line starch agreed with the SEM images of the RS residues. The RS residue of the existing *ae*-line starch displayed gel-like structure (Fig. 2C), which appeared amorphous, whereas that of the GEMS-0067 *ae*-line starch retained the granular structure (Fig. 2A), which had similar percentages of crystallinity to the native GEMS-0067 *ae*-line starches.

Although all the RS residues displayed the B-type X-ray diffraction pattern, the sharpness of the peaks at 14.5°, 21.9°, and 23.7° was reduced (Fig. 7B). This could be the result of the decrease in the crystallite size and distortion of the arrangement of the smaller

starch-crystallites in the granule during enzymatic hydrolysis at 95–100 °C. The absence of the V-type X-ray diffraction patterns with 2θ peaks at 8°, 13°, and 20° in the native starch and the RS residue (Zobel, 1988; Zobel, French, & Hinkle, 1967) showed that lipids present in the starch granule were not in a crystalline amylose–lipid complex.

4. Conclusions

The GEMS-0067 *ae*-line starches had substantially larger proportions of rod/filamentous starch granules (22.6–32.0%) than did the existing *ae*-line starches (5.2–7.7%). The rod/filamentous starch granules and the outer layer of the spherical starch granules were more resistant to enzymatic hydrolysis at 95–100 °C and remained in the RS residues. All the RS residues displayed the B-type polymorph and had gelatinization temperatures above 100 °C. All the RS residues consisted of two major components: large molecules (average DP 840–951) of mostly partially preserved amylose and IC molecules, and small molecules (average DP 59–74) of mostly linear chains resulting from enzymatic hydrolysis of semi-crystalline amylose, IC, and amylopectin molecules at 95–100 °C. The long-chain double-helical crystallites of amylose/IC molecules in the native *ae*-line starches, which had gelatinization temperature above 100 °C, retained the semi-crystalline structures and were resistant to the enzymatic hydrolysis at 95–100 °C. Lipids present in the granule also protected starch from enzymatic hydrolysis at 95–100 °C.

Acknowledgements

The authors thank the USDA-ARS GEM project for the support on this research, Microscopy and Nanolmaging Facility at Iowa State University for the microscopic study, and Dr. Schlörholtz for help on X-ray analysis.

References

- AO, Z., & Jane, J. (2007). Characterization and modeling of the A- and B-granule starches of wheat, triticale, and barley. *Carbohydrate Polymers*, 67, 46–55.
- AOAC. (2003). Association of Official Analytical Chemists (AOAC) Official Method 991.43. Total, soluble, and insoluble dietary fiber in foods. In W. Horwitz (Ed.), *Official methods of analysis of the AOAC international*. Gaithersburg, Maryland: AOAC International.
- Boyer, C. D., Daniels, R. R., & Shannon, J. C. (1976). Abnormal starch granule formation in Zea-Mays-L endosperms possessing amylose-extender mutant. *Crop Science*, 16, 298–301.
- Campbell, M. R., Jane, J., Pollak, L., Blanco, M., & O'Brien, A. (2007). Registration of maize germplasm line GEMS-0067. *Journal of Plant Registrations*, 1, 60–61.
- Dubois, M., Gilles, K. A., Hamilton, J. K., Rebers, P. A., & Smith, F. (1956). Colorimetric method for determination of sugars and related substances. *Analytical Chemistry*, 28, 350–356.
- Englyst, H. N., Kingman, S. M., & Cummings, J. H. (1992). Classification and measurement of nutritionally important starch fractions. *European Journal of Clinical Nutrition*, 46(Suppl. 2), S33–S50.
- Evans, A., & Thompson, D. B. (2004). Resistance to α-amylase digestion in four native high-amylose maize starches. *Cereal Chemistry*, 81, 31–37.

- French, D. (1984). Organization of starch granules. In R. L. Whistler, J. N. Bemiller, & E. F. Paschall (Eds.), *Starch: Chemistry and technology* (pp. 183–247). New York: Academic Press.
- Gray, J. A., & BeMiller, J. N. (2004). Development and utilization of reflectance confocal laser scanning microscopy to locate reaction sites in modified starch granules. *Cereal Chemistry*, 81, 278–286.
- Huber, K. C., & BeMiller, J. N. (2001). Location of sites of reaction within starch granules. *Cereal Chemistry*, 78, 173–180.
- Jane, J., & Chen, J. F. (1992). Effect of amylose molecular size and amylopectin branch chain length on paste properties of starch. *Cereal Chemistry*, 69, 60–65.
- Jane, J., & Robyt, J. F. (1984). Structure studies of amylose-V complexes and retrograded amylose by action of alpha amylases, and a new method for preparing amyloextrins. *Carbohydrate Research*, 132, 105–118.
- Jane, J., & Shen, J. J. (1993). Internal structure of the potato starch granule revealed by chemical gelatinization. *Carbohydrate Research*, 247, 279–290.
- Jane, J., Xu, A., Radosavljevic, M., & Seib, P. A. (1992). Location of amylose in normal starch granules: I. Susceptibility of amylose and amylopectin to cross-linking reagents. *Cereal Chemistry*, 69, 405–409.
- Kasemsuwan, T., Jane, J., Schnable, P., Stinard, P., & Robertson, D. (1995). Characterization of the dominant mutant amylose-extender (Ae1-5180) maize starch. *Cereal Chemistry*, 72, 457–464.
- Li, L., Blanco, M., & Jane, J. (2007). Physicochemical properties of endosperm and pericarp starches during maize development. *Carbohydrate Polymers*, 67, 630–639.
- Li, L., Jiang, H., Campbell, M., Blanco, M., & Jane, J. (2008). Characterization of maize amylose-extender (ae) mutant starches: Part I. Relationship between resistant starch contents and molecular structures. *Carbohydrate Polymers*, 74, 396–404.
- Mercier, C., Charbonniere, R., Gallant, D., & Guilbot, A. (1970). Development of some characteristics of starches extracted from normal corn and amylomaize grains during their formation. *Starch/Stärke*, 22, 9–16.
- Morell, M. K., Samuel, M. S., & O'Shea, M. G. (1998). Analysis of starch structure using fluorophore-assisted carbohydrate electrophoresis. *Electrophoresis*, 19, 2603–2611.
- Pan, D. D., & Jane, J. (2000). Internal structure of normal maize starch granules revealed by chemical surface gelatinization. *Biomacromolecules*, 1, 126–132.
- Schoch, T. J. (1942). Noncarbohydrate substances in the cereal starches. *Journal of the American Chemical Society*, 64, 2954–2956.
- Shi, Y.-C., Capitani, T., Trzasko, P., & Jeffcoat, R. (1998). Molecular structure of a low-amylopectin starch and other high-amylose maize starches. *Journal of Cereal Science*, 27, 289–299.
- Shi, Y.-C., & Jeffcoat, R. (2001). Structural features of resistant starch. In B. McCleary & L. Prosky (Eds.), *Advanced dietary fibre technology* (pp. 430–439). Oxford, UK: Wiley-Blackwell.
- Sidebottom, C., Kirkland, M., Strongitharm, B., & Jeffcoat, R. (1998). Characterization of the difference of starch branching enzyme activities in normal and low-amylopectin maize during kernel development. *Journal of Cereal Science*, 27, 279–287.
- Sievert, D., & Pomeranz, Y. (1990). Enzyme-resistant starch: II. Differential scanning calorimetry studies on heat-treated starches and enzyme-resistant starch residues. *Cereal Chemistry*, 67, 217–221.
- Takeda, C., Takeda, Y., & Hizukuri, S. (1989). Structure of amylomaize amylose. *Cereal Chemistry*, 66, 22–25.
- Wolf, M. J., Seckinger, H. L., & Dimler, R. J. (1964). Microscopic characteristics of high-amylose corn starches. *Starch/Stärke*, 16, 377–382.
- Yoo, S.-H., & Jane, J. (2002). Molecular weights and gyration radii of amylopectins determined by high-performance size-exclusion chromatography equipped with multi-angle laser-light scattering and refractive index detectors. *Carbohydrate Polymers*, 49, 307–314.
- Zobel, H. F. (1988). Starch crystal transformations and their industrial importance. *Starch/Stärke*, 40, 1–7.
- Zobel, H. F., French, A. D., & Hinkle, M. E. (1967). X-ray diffraction of oriented amylose fibers: II. Structure of V-amyloses. *Biopolymers*, 5, 837–845.